EPJ A
Hadrons and Nuclei

EPJ.org
your physics journal

Eur. Phys. J. A **43**, 153–158 (2010) DOI: 10.1140/epja/i2010-10906-2

^{6}He + ^{9}Be reactions at 16.8 MeV

M. Majer, R. Raabe, M. Milin, C. Angulo, J. Cabrera, E. Casarejos, J.L. Charvet, D. Escrig, A. Gillibert, Th. Keutgen, V. Lapoux, L. Nalpas, A. Ninane, A. Obertelli, N.A. Orr, F. Skaza, J.L. Sida, S.I. Sidorchuk, D. Smirnov and R. Wolski

EDP SCIENCES Società Italiana di Fisica Springer

Eur. Phys. J. A **43**, 153–158 (2010)
DOI 10.1140/epja/i2010-10906-2

THE EUROPEAN PHYSICAL JOURNAL A

Regular Article – Experimental Physics

^{6}He + ^{9}Be reactions at 16.8 MeV

M. Majer[1,a], R. Raabe[2], M. Milin[1,b], C. Angulo[3], J. Cabrera[4], E. Casarejos[4], J.L. Charvet[5], D. Escrig[6], A. Gillibert[5], Th. Keutgen[4], V. Lapoux[5], L. Nalpas[5], A. Ninane[4], A. Obertelli[5], N.A. Orr[7], F. Skaza[5], J.L. Sida[5], S.I. Sidorchuk[8], D. Smirnov[9], and R. Wolski[8,10]

[1] Department of Physics, Faculty of Science, University of Zagreb, HR-10000 Zagreb, Croatia
[2] GANIL, CEA/DSM - CNRS/IN2P3, Bd. Henri Becquerel, BP 55027, F-14076 Caen Cedex 5, France
[3] Tractebel Engineering, Avenue Ariane 7, B-1200 Brussels, Belgium
[4] Centre de Recherches du Cyclotron, Université Catholique de Louvain, B-1348 Louvain-la-Neuve, Belgium
[5] CEA-Saclay, DSM/IRFU/SPhN, F-91191 Gif-sur-Yvette Cedex, France
[6] Instituto de Estructura de la Materia, CSIC, E-28040 Madrid, Spain
[7] LPC-Caen, ENSICAEN, Université de Caen, CNRS/IN2P3, F-14050 Caen Cedex, France
[8] Flerov Laboratory of Nuclear Reactions, JINR, RU-141980 Dubna, Russia
[9] Instituut voor Kern-en Stralingsfysica, K.U. Leuven, B-3001 Leuven, Belgium
[10] Institute of Nuclear Physics, PL-31342 Krakow, Poland

Received: 27 August 2009 / Revised: 17 November 2009
Published online: 9 January 2010 –
Communicated by B.R. Fulton

Abstract. Reactions of a 16.8 MeV ^{6}He beam with a ^{9}Be target have been investigated using highly segmented detector setup covering a large solid angle. Data on elastic and quasi-free scattering, as well as two-neutron transfer, are reported. The results for elastic scattering are fairly well reproduced by a CDCC calculation, in agreement with the interpretation of a breakup effect already observed for the scattering of ^{6}He on other light targets. Exotic quasi-free scattering of ^{6}He on α-cluster in ^{9}Be is clearly observed. Inclusive and coincident events were used to extract information on the two-neutron transfer reaction ^{9}Be(^{6}He, α)^{11}Be. Sequential decay of the ^{11}Be state at the excitation energy E_x = 10.6 MeV through different channels is discussed.

1 Introduction

Elastic and inelastic scattering and transfer reactions induced by light nuclei are a major source of spectroscopic information. Selective population of states by transfer reactions can often give a straightforward insight into their structure. The use of radioactive beams, although experimentally demanding, allows these methods to be employed for nuclei far from the line of stability.

Reactions induced by ^{6}He have attracted considerable interest as it is the lightest two-neutron halo nucleus [1]. Measurements at various energy ranges have shown the importance of the role played by the continuum in the reaction mechanism and its effects on the elastic scattering and fusion probabilities [2–6]. Experimental data are, however, still rather scarce (see, *e.g.* [6], for a recent review), especially at low energies, so further measurements are very welcome.

In the present work, the choice of the target (^{9}Be) was primarily motivated by the aim of studying the ^{7}He. The nucleus ^{9}Be is a rather deformed and loosely bound system which is amenable to a cluster or molecular model description. For example, the ground state of ^{9}Be is described as two clusters ($\alpha + {}^5$He) in the $L = 0$ relative motion (see *e.g.* refs. [7,8]). The first three states of the ground-state rotational band are clearly identified, while the fourth one is still under discussion (see, *e.g.* ref. [7]) —unfortunately, the beam energy in this experiment was too small to study that state. Other known states in ^{9}Be also show prominent clustering; actually, most of them fit the so-called "molecular" picture in which valence neutrons fill different molecular orbitals around two α-particles [9,10]. Such an exotic structure makes ^{9}Be a good target for studies of cluster and molecular states in heavier beryllium isotopes, as well as other light nuclei.

The ^{6}He + ^{9}Be reactions were previously investigated only at 150 MeV [11,12]. Differential cross-sections were reported for quasi-elastic scattering, breakup reaction and 1n- and 2n-transfer reactions. Angular distribution for the ^{6}He + ^{9}Be elastic scattering at $E \approx 9$ MeV is given in [13].

In this work we report the results for the reactions of a 16.8 MeV ^{6}He beam on a ^{9}Be target. These results were obtained as part of an experiment designed to probe the structure of ^{7}He via the ^{9}Be(^{6}He, ^{8}Be)^{7}He reaction [14].

[a] e-mail: marija@phy.hr
[b] e-mail: matko.milin@phy.hr

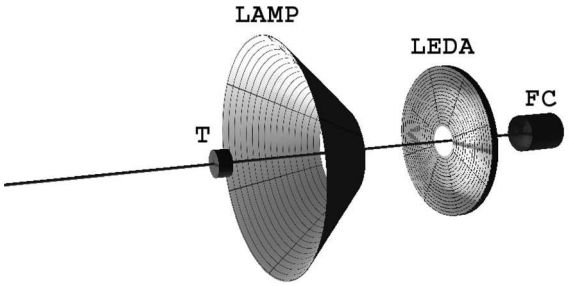

Fig. 1. Schematic view of the experimental setup. The positions of the target and Faraday cup are indicated with "T" and "FC", respectively. LEDA and LAMP are silicon strip detector arrays described in text.

2 Experiment

The experiment was performed at the Cyclotron Research Center (CRC), the radioactive beam facility in Louvain-la-Neuve [15,16]. The experimental setup is given in fig. 1. The 16.8 MeV $^6He^+$ beam was produced by the Isotope-Separation-on-Line technique using two coupled cyclotrons. The average intensity of the beam on the Be-target was about 10^7 pps for a total irradiation time of about five days. The beam purity was excellent —the only impurity observed was a very small contribution of the HeH_2^+ ions [17]. The target used was a 400 μg/cm^2 thick self-supporting foil of ^{9}Be manufactured at the Laboratori Nazionali del Sud (Catania, Italy). For calibration and normalisation purposes, an Au target 200 μg/cm^2 thick was also used.

Outgoing charged particles were detected in 224 silicon strip detectors arranged in the two large detector arrays [18]. The forward-angle detector array (LEDA, Louvain-Edinburgh Detector Array) consisted of 8 segments each containing 16 strips, 300 μm thick. The polar angles covered were 4°–12° and the azimuthal range was 0–360°. The second detector array (called LAMP because of its lampshade geometry) had 6 segments of LEDA-type detectors (each segment was inclined 45°) and was placed closer to the target to cover larger polar angles (22°–72°) and also the full azimuthal range. The energy calibration of detectors was performed with the three-peaks-alpha-source and elastic scattering of ^{6}He on the gold target. The intrinsic energy resolution was $\approx$ 25 keV.

Particle identification was performed by the time of flight (ToF) method. A typical ToF *vs.* energy spectrum for a single strip at $\theta = 11.3°$ is displayed in fig. 2. The mass resolution obtained for LEDA was good enough to separate α-particles from ^{6}He nuclei, while in LAMP the small distance to the target resulted in a poor mass separation. For some coincidence events, identification of outgoing particles detected in LAMP was achieved by kinematic reconstruction (by calculating the so-called kinematical mass from the energy and angle of detected particles).

The total collected charge was monitored by a Faraday cup —its reading was normalised with a measurement of elastic scattering of ^{6}He on the thin gold target (purely Rutherford at the beam energy used). The FWHM of the elastic peak recorded in a single strip in LEDA was around 60 keV, larger than the intrinsic energy resolution of the detector —this was due to the beam energy spread and straggling from energy loss in the target. An additional enlargement occurred for the measurement on ^{9}Be due to the finite polar angle covered by each strip (which was much larger in LAMP than in LEDA).

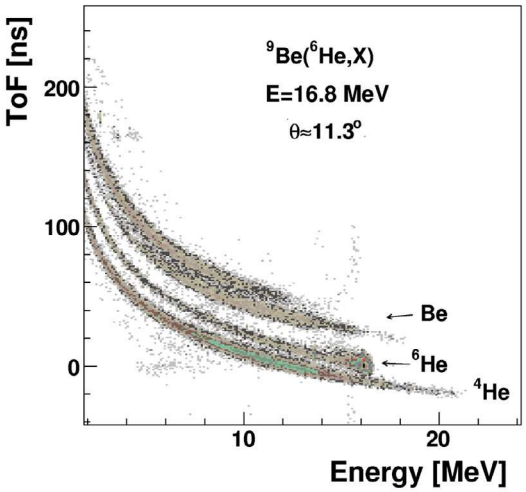

Fig. 2. Time-of-flight (ToF) *vs.* energy spectrum for one of the strips in the LEDA detector array.

3 Results

3.1 Elastic scattering

There are only a few measurements of the ^{6}He elastic scattering on light targets at low energies. The first data, measured at $E \approx 9$ MeV on several targets [13], could be reproduced using optical model parameters from ^{6}Li and ^{7}Li rather than parameters from ^{4}He. The same behaviour was observed for the ^{6}He scattering on ^{12}C [19] and ^{6,7}Li at $E = 18$ MeV [20]. For these targets a direct comparison of the actual scattering data for the ^{6}He and ^{6}Li projectiles is found in the latter two publications. Comparison of data for the scattering of ^{6}He and ^{6}Li projectiles on a ^{4}He target at $E_{\rm cm} \approx 11$ MeV is found in ref. [21]. In all cases, the data show strong similarities, leading to the conclusion that the reaction mechanism for the two projectiles was similar.

Differences appeared, on the other hand, for the elastic scattering on heavier targets like ^{208}Pb [4]. They were explained as the effect of projectile breakup into an α-particle and two neutrons (for ^{6}He) or a deuteron (for ^{6}Li). On heavy targets, the part of the breakup due to the Coulomb field acts differently on the two projectiles.

The coupling of breakup to elastic scattering remains, however, important also for light targets (in this case, the nuclear field is the prominent one). This was shown in refs. [21] and [22], where the ^{6}He + ^{4}He and the ^{6}Li + ^{4}He

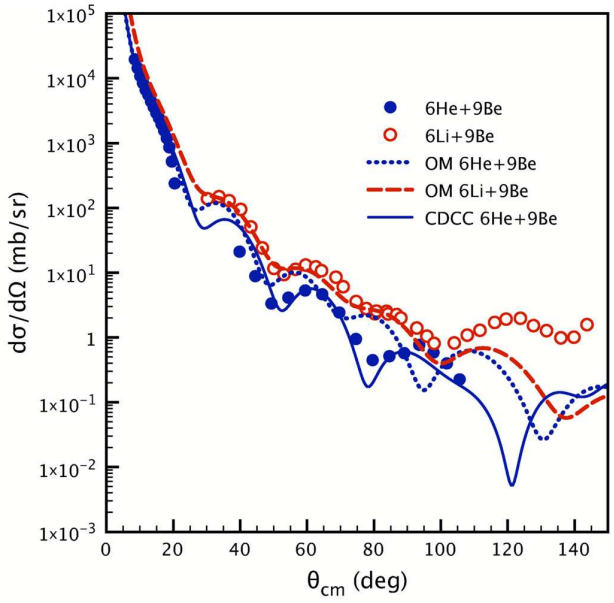

Fig. 3. Experimental angular distribution for the ^{6}He + ^{9}Be elastic scattering measured at $E = 16.8$ MeV (full circles), compared with data for the ^{6}Li + ^{9}Be scattering at $E = 16.6$ MeV [25] (open circles). The dotted and dashed curves are optical model fits of the ^{6}He + ^{9}Be and ^{6}Li + ^{9}Be data, respectively. The solid curve is a calculation for the ^{6}He + ^{9}Be elastic scattering that takes into account the breakup of the ^{6}He projectile using the CDCC method. Error bars are smaller than the size of data points as plotted.

scattering data were reproduced by calculations in which the projectile breakup channel was taken into account by using the continuum-discretised coupled-channel method (CDCC) and, more recently, in ref. [23], where a four-body CDCC calculation, which included a three-body description of the Borromean ^{6}He nucleus, managed to obtain a good agreement with the ^{6}He + ^{12}C data at $E = 18$ MeV. Coupling to the breakup channel could also be invoked to explain the discrepancy between the high-quality ^{6}He + ^{12}C scattering data at 10.2 MeV and the optical model fit (using ^{6}Li parameters) in ref. [24], however the calculations in this case were not made.

Our experimental angular distribution for the ^{6}He + ^{9}Be elastic scattering is given in fig. 3. At small angles, the data points were obtained from the number of events in the elastic peak in inclusive spectra of both detector arrays. At larger angles, where the peak was not immediately visible, LAMP-LAMP coincidence events identified through kinematic reconstruction were used. The efficiency of coincidence detection of such events has been obtained by Monte Carlo simulations. In the overlapping region agreement between the data points obtained with the two methods was very good and the final result (shown in fig. 3) is obtained as the weighted average. An additional systematic uncertainty of about 10% is related to the normalization performed with the Au target.

Experimental data for the ^{6}Li + ^{9}Be elastic scattering at 16.6 MeV [25] are also shown in the same figure. As expected from the arguments presented above, the two data sets exhibit similar behaviour. Optical model fits were performed, based on existing parameters for the ^{6}Li + ^{9}Be system at 32 MeV [26]. In the fit, the depth of the real and imaginary parts of the potential were allowed to vary (a fit varying the radius and diffuseness parameters did not lead to physically meaningful results).

The resulting curves (fig. 3) start to differ from the data at angles beyond $\theta_{\rm cm} \approx 100°$ for ^{6}Li, and already at $\theta_{\rm cm} \approx 70°$ for ^{6}He. For the ^{6}He + ^{9}Be scattering, a CDCC calculation was also performed using the version FRXY.4a of the code FRESCO [27]. The ^{6}He continuum above the $\alpha + 2$n breakup threshold was discretized into momentum bins with the same scheme used by the authors in ref. [21], but taking into account the whole momentum space. The di-neutron model from ref. [21] is known to overestimate the effect of breakup for heavy targets [28]; however in the present case, where nuclear forces dominate, we expect essentially no difference with respect to the more refined model of ref. [28]. For the ^{4}He-^{9}Be interaction, required by the calculation, the potential reported in ref. [29] was used. The result of the calculation was not very sensitive to the parameters of the ^{9}Be-2n scattering potential, for which a scan was performed; eventually, real and imaginary potential depths $V = -50$ MeV and $W = -17$ MeV were used, with radius $r = 1.4$ fm and diffuseness $a = 0.5$ fm. With the CDCC method, thus including the effect of the projectile breakup channel, the agreement with the experimental data was improved. The total reaction cross-section, as given by the CDCC calculation, is 1436 mb.

The transfer channel, and in particular the 1n- and 2n-transfer from the ^{6}He projectile, could also play a role in the reaction mechanism. However a more sophisticated calculation, beyond the scope of this article, would be necessary to assess the extent of such effects on the elastic scattering. Even if somewhat partial, however, the results that we obtained in the CDCC framework support previous observations of an effect of the breakup channel on the elastic scattering of light weakly bound nuclei at these low energies (see, for example, ref. [30]).

3.2 Quasi-free scattering

In the quasi-free scattering (QFS), one of the nuclei in the collision scatters on the cluster in another nucleus and ejects that cluster from the parent nucleus. If the scattering happens on the cluster in the target nucleus, the remaining "spectator" is assumed to have an energy close to zero (actually, the energy of the spectator depends on the relative motion of the clusters in the nucleus and for $L > 0$ it can range up even to a couple of hundred keV). As such, although there are three particles in the final state, two-body kinematics can be applied (including the condition that two outgoing particles should have $\Delta\phi \approx 180°$). In this manner, particle identification becomes possible in the present experiment for coincidence events, even for the LAMP detector where the ToF method cannot be applied.

The nucleus ^{9}Be is known to have a well-developed cluster structure in the ground state which leads to

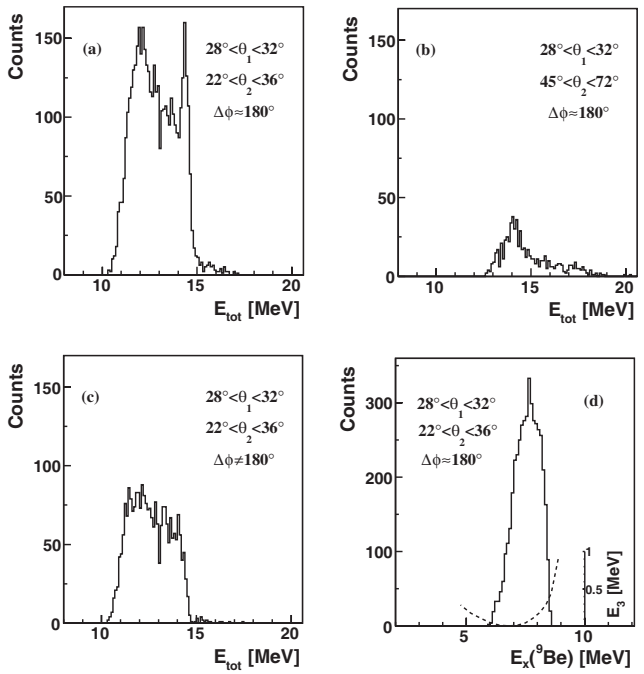

Fig. 4. Total energy for the ^{6}He+α coincidences selected with both particles detected in LAMP and for (a) quasi-free angles: $28^\circ < \theta_1 < 32^\circ$, $22^\circ < \theta_2 < 36^\circ$, $\Delta\phi \approx 180^\circ$; (b) polar angles not fulfilling quasi-free conditions; (c) azimuthal angles not fulfilling quasi-free conditions. (d) The ^{9}Be excitation energy for the events from panel (a) of this figure. The dashed line gives the energy of the third (undetected) particle with the energy scale given at the right side of the figure.

pronounced scattering of stable projectiles on one of the α-clusters in ^{9}Be, as observed in a number experiments. In most of the QFS measurements with a ^{9}Be target, the $(\alpha, 2\alpha)$ reaction was studied [31–33], while there are also some results for the $(\mathrm{p}, \mathrm{p}\alpha)$ reaction [34,35].

On the other hand, QFS of weakly bound projectiles, especially those having low energy, is an interesting subject to study. Particularly, for such projectiles, QFS is expected to be suppressed by other processes (mainly breakup). Surprisingly, it has been found that the weakly bound nucleus ^{7}Li at $E = 52$ MeV can undergo quasi-free scatter from ^{9}Be [36]. Furthermore, quasi-free scattering of an even more weakly bound (and radioactive) projectile, ^{6}He, on the deuteron cluster in ^{6}Li has been recently claimed [37,38] for the $^6\mathrm{He} + {}^6\mathrm{Li}$ system at $E = 18$ MeV. This claim can be further strengthened by the observation of QFS in the $^6\mathrm{He} + {}^9\mathrm{Be}$ system.

Figures 4(a)–(c) show the total energy of two particles detected in LAMP for different angular regions. Two-body kinematic conditions (corresponding to the ^{6}He and α as outgoing particles after QFS) were applied to select events shown in spectrum (a). Figures 4(b) and (c) were obtained without applying the QFS conditions for polar and azimuthal angles, respectively. A clear difference between the total energy spectra in figs. 4(a)–(c) is the strong peak visible at $E_{\mathrm{tot}} \approx 14.3$ MeV in panel (a) which is absent in (b) and (c). Two-body exit channels could not produce a peak seen in fig. 4(a). Since the Q-value of the $^6\mathrm{He} + \alpha$ QFS is -2.5 MeV (corresponding to the α-particle separation energy in ^{9}Be) and the remaining, undetected particles carry only a very small kinetic energy, one can conclude that the peak is produced by the $^6\mathrm{He} + \alpha$ QFS.

To confirm that the $^6\mathrm{He} + 2\alpha + \mathrm{n}$ exit channel is reached through QFS and *not* through sequential decay of states in ^{9}Be, ^{10}Be and ^{11}Be, one has to check all relative energy spectra between particles in the exit channel. Panel (d) of fig. 4 shows that the events in (a) do *not* arise from sequential decay through the states in ^{9}Be because they would correspond to an excitation energy centred at $E_x(^9\mathrm{Be}) \approx 7.5$ MeV (as calculated from energy and angle of detected ^{6}He) where there are no ^{9}Be states that decay via α-emission [7]. Similarly, it has been verified (from the energy and angle of the detected α-particle) that the quasi-free peak in fig. 4(a) corresponds to $E_x(^{11}\mathrm{Be}) \approx 11$–$14$ MeV and that it is not caused by the sequential decay of states in ^{11}Be. Finally, in the ^{10}Be excitation energy spectrum, the quasi-free peak appears as a broad bump at $E_x(^{10}\mathrm{Be}) > 10.9$ MeV. The $^6\mathrm{He} + \alpha$ cluster structure of ^{10}Be has been extensively studied in recent years and such states are now well established [39–41] —it is known that in the region $E_x(^{10}\mathrm{Be}) > 10.9$ MeV there are *no* states that can produce such a strong peak as the one given in fig. 4(a).

All these arguments give clear evidence to claim observation of QFS of the ^{6}He projectile on the α-cluster in ^{9}Be. This is consistent with a previous observation for the $^6\mathrm{He} + {}^6\mathrm{Li}$ system [37,38], which is to our knowledge the only report of QFS of a weakly bound radioactive projectile on a cluster in target nuclei. The value of this (only qualitative) observation is not in studying the structure of the target nucleus (^{9}Be) which can be better done with stable beams, but rather in opening a possibility to apply QFS to learn something about neutron scattering on neutron-rich nuclei (by the use of radioactive nuclear beams and, *e.g.*, deuterons as neutron target).

3.3 The $^6\mathrm{He} + {}^9\mathrm{Be} \rightarrow \alpha + {}^{11}\mathrm{Be}$ reaction

In a series of measurement by the Berlin group [42–45], it was shown that transfer of two (or three) neutrons onto a ^{9}Be target populates a large number of states in ^{11}Be (^{12}Be) up to high excitation energies, contrary to the measurements with the ^{10}Be target where only low-lying states are populated. Based on these results, the existence of a rotational band in ^{11}Be was suggested [9,42–46], with a deformation comparable to that of a recently established band of extremely deformed states in ^{10}Be [39,40]. Theoretical calculations in the framework of antisymmetrised molecular dynamics [47] provide strong support for the existence of such states, while the microscopic multicluster model (involving $2\alpha+3$n configurations) does not support this conjecture [48]. Large-basis *ab initio* shell model investigation of ^{11}Be has also been performed [49], reproducing the spectrum of the low-lying ^{11}Be states. A very recent experimental study of the $^9\mathrm{Be}(^{16}\mathrm{O}, {}^{14}\mathrm{O})$ reaction [50]

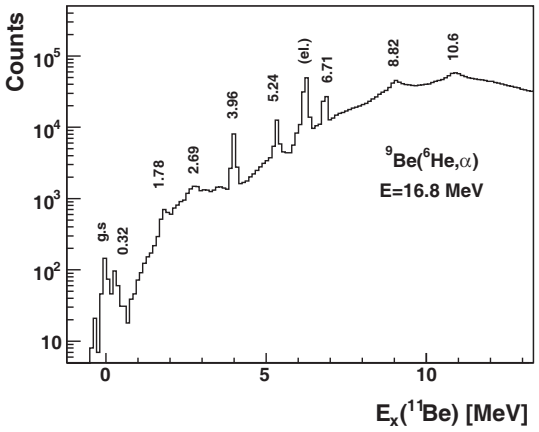

Fig. 5. ^{11}Be excitation energy spectrum derived from the energies of the α-particles detected in LEDA. FWHM of the ground state is about 140 keV mostly due to finite size of the detector strips as discussed in text.

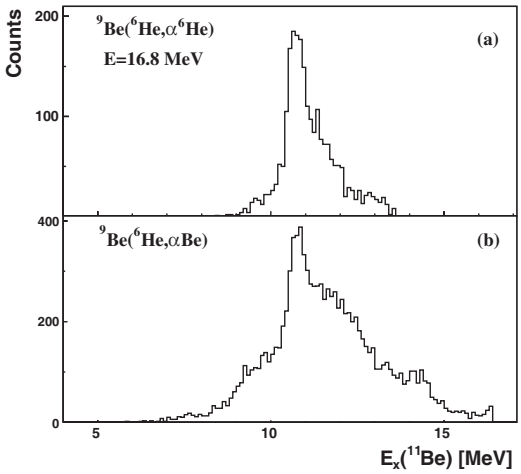

Fig. 6. ^{11}Be excitation energy spectrum extracted from the LEDA-LEDA coincidence events with particles having $A = 4$ and $A = 6$ (upper panel) and $A = 4$ and $A = 9$–10 (lower panel).

with sequential neutron decay of the populated ^{11}Be states furnished further data on states up to $E_x = 8.82$ MeV.

Figure 5 displays the ^{11}Be excitation energy spectrum for the ^{9}Be(^{6}He, ^{4}He)^{11}Be reaction with α-particles detected in LEDA (single events). This spectrum resembles more closely those obtained [42–45] with the two-neutron transfer reactions with heavier projectiles (^{13}C, ^{14}N, ^{16}O) at much higher energies, than to the spectrum obtained through the ^{9}Be(t, p) reaction at 20 MeV [51, 52]. In addition, our spectrum exhibits a more pronounced background arising principally from ^{6}He breakup. This background is strongly suppressed for the coincidence events, as shown in fig. 6. Eight peaks in ^{11}Be can be clearly identified in fig. 5: apart of the ground state ($3/2^-$), these peaks correspond to the states at E_x = 0.32 MeV ($1/2^-$), 1.78 MeV ($5/2^+$), doublet at $\approx$ 3.9 MeV, 5.24 MeV, 6.71 MeV, 8.82 MeV, and 10.6 MeV (the spins and parities of the last three states are not yet established). The state at $E_x = 2.69$ MeV ($3/2^-$) also seems to be weakly populated in fig. 5. A peak at $E_x(^{11}\mathrm{Be}) \approx 6.2$ MeV corresponds to the elastic scattering, not completely suppressed by the gate in the ToF *vs.* E spectrum (fig. 2).

Figure 6 displays the ^{11}Be excitation energy spectrum extracted from the LEDA-LEDA coincidence events with particles of $A = 4$ and $A = 6$ (upper panel) or $A = 4$ and $A = 9$–10 (lower panel). The high-energy α-particle arise from the first step (*i.e.* the ^{9}Be(^{6}He, α)^{11}Be reaction), and the excitation energy spectrum is calculated from the detected energy and angle of that particle. The ^{6}He or ^{9,10}Be nuclei (the ^{9}Be and ^{10}Be events were not clearly resolved) arise from the sequential decay of the ^{11}Be states. A strong peak that dominates both spectra in fig. 6 corresponds to the known ^{11}Be state at $E_x(^{11}\mathrm{Be}) \approx 10.6$ MeV (listed as $E_x(^{11}\mathrm{Be}) = 10.71$ MeV in ref. [50]). The same ^{11}Be state is seen also in the $\alpha + \alpha$ coincidences (both particles in LEDA). With the obtained results it is not possible to determine through which of the sequential channels (^{10}Be* + n, ^{7}He + α or ^{6}He + ^{5}He) this state decays.

A comparison of the number of counts in the $E_x(^{11}\mathrm{Be}) = 10.6$ MeV peak in the two spectra in fig. 6 gives a factor of 1.83 more counts for the ^{9}Be(^{6}He, αBe) case. A simple Monte Carlo simulation taking into account only the geometry of detectors (and not the details of decay angular distributions) gives the detection efficiency for the two discussed exit channels (^{6}He + α + n and ^{9}Be + 2n) same within 15%. Therefore, if the ^{10}Be states are involved in sequential decay, those have to be the states which show comparable decay strengths through both the ^{9}Be + n and the ^{6}He + α channels —there is only one such state known in ^{10}Be and that is the 2^+ state at $E_x(^{10}\mathrm{Be}) \approx 9.56$ MeV [39, 53, 54].

This conclusion agrees with the results of the ^{11}Li β-decay studies [55–58] that there is a significant β-decay branch to the $E_x(^{11}\mathrm{Be}) = 10.6$ MeV state, which then decays by neutron emission to one of the states at $E_x(^{10}\mathrm{Be}) \approx 9.3$–9.6 MeV (now known to be the 2^+ state at 9.56 MeV) and then to either the ^{6}He + α channel [56] or ^{9}Be + n channel [55, 57]. It is interesting to note that the discussed ^{11}Be state is around 10.1 MeV above the ^{10}Be + n threshold, and this is just equal to the excitation energy of the recently established 4^+ molecular state in ^{10}Be [39, 40]. This, and the fact that is strongly populated in the β-decay of the halo nucleus ^{11}Li, indicates that the 10.6 MeV state in ^{11}Be has a very special structure, probably with well developed clustering. Studying reactions with other radioactive projectiles, like ^{7}Li(^{8}Li, α)^{11}Be (Q = 13.3 MeV) or ^{13}C(^{6}He, ^{8}Be)^{11}Be ($Q = -4.4$ MeV), could give further information on the structure of this very interesting state.

4 Conclusions

The first experimental results for the ^{6}He + ^{9}Be reactions measured at low energy (E = 16.8 MeV) are presented. The elastic scattering data is compared with scattering on

a ^{6}Li target at a similar energy and with CDCC calculations which suggest that breakup plays a role even at these low beam energies. The ^{6}He quasi-free scattering off the α-cluster in ^{9}Be is clearly observed, confirming the claim [37, 38] that even spatially extended and very weakly bound nuclei can undergo such scattering. The two-neutron stripping reaction, ^{9}Be(^{6}He, ^{4}He)^{11}Be, is investigated and the ^{11}Be excitation energy spectra are derived from inclusive and coincidence events. States suggested [9, 42–45] to have a strong deformation and to belong to a rotational band are selectively populated and for one of these states (at 10.6 MeV), the sequential emission of α-particles, ^{6}He and Be nuclei has been observed.

We would like to thank the technical staff at the RNB facility at the CRC-Louvain-la-Neuve for their valuable contributions to this work.

References

1. M.V. Zhukov *et al.*, Phys. Rep. **231**, 151 (1993).
2. V. Lapoux *et al.*, Phys. Lett. B **517**, 18 (2001).
3. V. Lapoux *et al.*, Phys. Rev. C **66**, 034608 (2002).
4. K. Rusek *et al.*, Phys. Rev. C **67**, 041604(R) (2003).
5. N. Keeley, R. Raabe, N. Alamanos, J.L. Sida, Prog. Part. Nucl. Phys. **59**, 579 (2007).
6. N. Keeley, N. Alamanos, K.W. Kemper, K. Rusek, Prog. Part. Nucl. Phys. **63**, 396 (2009).
7. N. Soić *et al.*, Europhys. Lett. **41**, 489 (1998).
8. N. Keeley, K.W. Kemper, K. Rusek, Phys. Rev. C **64**, 031602 (2001).
9. W. von Oertzen, M. Freer, Y. Kanada-En'yo, Phys. Rep. **432**, 43 (2006).
10. M. Freer, Rep. Prog. Phys. **70**, 2149 (2007).
11. Y.L. Ye *et al.*, Phys. Rev. C **71**, 014604 (2005).
12. Y.L. Ye *et al.*, J. Phys. G **31**, S1647 (2005).
13. R.J. Smith *et al.*, Phys. Rev. C **43**, 761 (1991).
14. R. Raabe *et al.*, in preparation.
15. D. Darquennes *et al.*, Phys. Rev. C **42**, R804 (1990).
16. G. Ryckewaert, J.M. Colson, M. Gaelens, M. Loiselet, N. Postiau, Nucl. Phys. A **701**, 323c (2002).
17. Đ. Miljanić, M. Milin *et al.*, Nucl. Instrum. Methods: Phys. Res. A **447**, 544 (2000).
18. T. Davinson *et al.*, Nucl. Instrum. Methods: Phys. Res. A **454**, 350 (2000).
19. M. Milin *et al.*, Nucl. Phys. A **730**, 285 (2004).
20. M. Milin *et al.*, Nucl. Phys. A **746**, 183c (2004).
21. K. Rusek, K.W. Kemper, Phys. Rev. C **61**, 034608 (2000).
22. K. Rusek *et al.*, Phys. Rev. C **56**, 1895 (1997).
23. T. Matsumoto *et al.*, Phys. Rev. C **70**, 061601 (2004).
24. R.E. Warner *et al.*, Phys. Rev. C **51**, 178 (1995).
25. E. Muskat *et al.*, Nucl. Phys. A **581**, 42 (1995).
26. J. Cook, K.W. Kemper, Phys. Rev. C **31**, 1745 (1985).
27. I.J. Thompson, Comput. Phys. Rep. **7**, 167 (1988).
28. A. Moro *et al.*, Phys. Rev. C **75**, 064607 (2007).
29. R.B. Taylor *et al.*, Nucl. Phys. A **65**, 318 (1965).
30. Y. Sakuragi *et al.*, Prog. Theor. Phys. (Jpn.), Suppl. **89**, 136 (1982).
31. A. Guichard *et al.*, Phys. Rev. C **4**, 700 (1971).
32. C.W. Wang *et al.*, Phys. Rev. C **21**, 1705 (1980).
33. A.A. Cowley *et al.*, Phys. Rev. C **50**, 2449 (1994).
34. P.G. Roos, H.G. Pugh, M. Jain, H.D. Holmgren, M. Epstein, C.A. Ludemann, Phys. Rev. **176**, 1246 (1968).
35. T. Yoshimura *et al.*, Nucl. Phys. A **641**, 3 (1998).
36. N. Soić *et al.*, Eur. Phys. J. A **3**, 303 (1998).
37. M. Milin *et al.*, Phys. At. Nucl. **69**, 1360 (2006).
38. Đ. Miljanić, M. Milin *et al.*, Europhys. Lett. **76**, 801 (2006).
39. M. Milin, M. Zadro *et al.*, Nucl. Phys. A **753**, 263 (2005).
40. M. Freer, E. Casarejos *et al.*, Phys. Rev. Lett. **96**, 042501 (2006).
41. M. Milin *et al.*, Europhys. Lett. **48**, 616 (1999).
42. H.G. Bohlen *et al.*, Phys. At. Nucl. **66**, 1494 (2003).
43. H.G. Bohlen *et al.*, Nucl. Phys. A **722**, 3c (2003).
44. H.G. Bohlen *et al.*, Nucl. Phys. A **734**, 345c (2003).
45. H.G. Bohlen, W. von Oertzen, A. Blažević, B. Gebauer, M. Milin, T. Kokalova, Ch. Schulz, S. Thummerer, A. Tumino, *Proceedings of the International Symposium on Exotic Nuclei, Lake Baikal, Russia, 2001*, edited by Yu.E. Penionzhkevich, E.A. Cherepanov (World Scientific, Singapore, 2002) p. 453.
46. H.G. Bohlen *et al.*, Phys. At. Nucl. **65**, 603 (2002).
47. Y. Kanada-En'yo, H. Horiuchi, Phys. Rev. C **66**, 024305 (2002).
48. P. Descouvemont, Nucl. Phys. A **699**, 463 (2002).
49. C. Forssén *et al.*, Phys. Rev. C **71**, 044312 (2005).
50. P.J. Haigh, M. Freer, N.I. Ashwood, T. Bloxham, N. Curtis, P. McEwan, H.G. Bohlen, T. Dorsch, Tz. Kokalova, Ch. Schulz, C. Wheldon, Phys. Rev. C **79**, 014302 (2009).
51. F. Ajzenberg-Selove *et al.*, Phys. Lett. B **40**, 205 (1972).
52. G.-B. Liu, H.T. Fortune, Phys. Rev. C **42**, 167 (1990).
53. N. Soić *et al.*, Europhys. Lett. **34**, 7 (1996).
54. N. Curtis *et al.*, Phys. Rev. C **64**, 044604 (2001).
55. M. Madurga, M.J.G. Borge *et al.*, Nucl. Phys. A **810**, 1 (2008).
56. M. Langevin *et al.*, Nucl. Phys. A **366**, 449 (1981).
57. Y. Hirayama, T. Shimoda, H. Izumi, A. Hatakeyama, K.P. Jackson, C.D.P. Levy, H. Miyatake, M. Yagi, H. Yano, Phys. Lett. B **611**, 239 (2005).
58. D.J. Morrissey *et al.*, Nucl. Phys. A **627**, 222 (1997).